Behavioural Brain Research 459 (2024) 114786

Contents lists available at ScienceDirect

Behavioural Brain Research

journal homepage: www.elsevier.com/locate/bbr

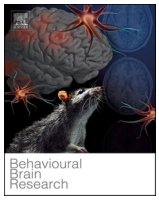

Research report

Enhanced anxiety-like behavior induced by chronic neuropathic pain and related parvalbumin-positive neurons in male rats

Thu Nguyen Dang [a], Son Nguyen Tien [b], Ryosuke Ochi [a], Duc Le Trung [a], Kyo Nishio [a], Hiroki Kuwamura [a], Tomoyuki Kurose [a], Naoto Fujita [a], Hisao Nishijo [c], Yoki Nakamura [d], Kazue Hisaoka-Nakashima [d], Norimitsu Morioka [d], Susumu Urakawa [a,*]

[a] *Department of Musculoskeletal Functional Research and Regeneration, Graduate School of Biomedical and Health Sciences, Hiroshima University, 1-2-3 Kasumi, Minami-ku, Hiroshima City, Hiroshima 734-8553, Japan*
[b] *Department of Rheumatology and Endocrinology, Military Hospital 103, Vietnam Military Medical University, No. 261 Phung Hung Street, Ha Dong District, Hanoi 12108, Viet Nam*
[c] *Faculty of Human Sciences, University of East Asia, 2-12-1 Ichinomiya Gakuen-cho, Shimonoseki City, Yamaguchi 751-8503, Japan*
[d] *Department of Pharmacology, Graduate School of Biomedical and Health Sciences, Hiroshima University, 1-2-3 Kasumi, Minami-ku, Hiroshima City, Hiroshima 734-8553, Japan*

ARTICLE INFO

Keywords:
Neuropathic pain
Anxiety-like behaviors
Parvalbumin-positive neurons
Corticolimbic regions

ABSTRACT

Anxiety commonly co-occurs with and exacerbates pain, but the interaction between pain progression and anxiety, and its underlying mechanisms remain unclear. Inhibitory interneurons play a crucial role in maintaining normal central nervous system function and are suggested to be involved in pain-induced anxiety. This study aimed to elucidate the time-dependent effects of neuropathic pain on the developmental anxiety-like behaviors and related inhibitory interneurons; parvalbumin (PV)- and cholecystokinin (CCK)-positive neurons in corticolimbic regions. Using an 8-week-old male Wistar rat model with partial sciatic nerve ligation (pSNL), anxiety-like behaviors were biweekly assessed post-surgery through open field (OF) and elevated plus maze (EPM) tests. From 4 weeks post-surgery, pSNL rats exhibited reduced OF center time, rearing, and initial activity, along with diminished EPM open-arm activities (time spent, head dips, movement, and rearing), which correlated with the paw withdrawal threshold. These effects were absent at 2 weeks post-surgery. At 8 weeks post-surgery, specific behaviors (decreased total rearing and increased inactive time in EPM) were observed in the pSNL group. Immunohistochemistry revealed changes in PV- and CCK-positive neurons in specific corticolimbic subregions of pSNL rats at 8 weeks post-surgery. Notably, PV-positive neuron densities in the basolateral amygdaloid complex (BLC) and hippocampal cornu ammonis areas 1 and 2 correlated with anxiety-like behavioral parameters. PV-positive neurons in the BLC of pSNL rats were predominantly changed in large-cell subtypes and were less activated. These findings indicate that anxiety-like behaviors emerge in the late phase of neuropathic pain and relate to PV-positive neurons in corticolimbic regions of pSNL rats.

1. Introduction

Pain is not only a significant health concern for the individual but also a social issue due to its diverse and multifaceted effects [1]. Chronic pain affects 11–40% of adults worldwide and the increase in incidence has been estimated at 8% per year [1]. Affective pain disorders, including anxiety, are common, with a comorbidity rate of up to 35% [2]. Individuals with chronic pain were four times more likely to

Abbreviations: PV, Parvalbumin; CCK, Cholecystokinin; pSNL, partial sciatic nerve ligation; OF, open field; EPM, elevated plus maze; GABA, Gamma-Amino Butyric Acid; PBS, Phosphate-buffered saline; PBS-T, PBS containing 0.25% Triton X-100; DAPI, 4′,6-Diamidino-2-phenylindole; AP, Anterior to posterior; CeA, Central amygdala; MeA, Medial amygdala; BLC, Basolateral amygdaloid complex; LA, Lateral amygdala; BLA, Basolateral amygdala; mPFC, Medial prefrontal cortex; ACC, Anterior cingulate cortex; PL, Prelimbic cortex; IL, Infralimbic cortex; CA, Cornu ammonis; DG, Dentate gyrus; S1, primary somatosensory cortex; FL, forelimb; HL, hindlimb; GI, granular insula, DI, dysgranular insula, AI, agranular insula; OLETF, Otsuka Long-Evans Tokushima fatty.

* Correspondence to: Department of Musculoskeletal Functional Research and Regeneration, Graduate School of Biomedical and Health Sciences, Hiroshima University, 1-2-3, Kasumi, Minami-ku, Hiroshima 734-8553, Japan.
E-mail address: urakawas@hiroshima-u.ac.jp (S. Urakawa).

https://doi.org/10.1016/j.bbr.2023.114786
Received 28 September 2023; Received in revised form 19 November 2023; Accepted 23 November 2023
Available online 29 November 2023

experience anxiety than those without chronic pain [3]. This combination of nociception and behavioral disorders impedes treatment and has a profound effect on the quality of life [4]. Effective pain and anxiety management requires a comprehensive understanding of the interactions within the central nervous system. Although this comorbidity is clinically well-established, the precise temporal indicators for the development of anxiety disorders in these pain phenotypes and the underlying mechanisms remain unknown.

Pain processing involves distinct structures that detect and respond to harmful stimuli, leading to complex behaviors [5]. Since spinal structures mediate primitive reflexes, higher brain centers—such as the amygdala, hippocampus, and cortical areas including the medial prefrontal, insular, and somatosensory cortices—manage conscious processing and emotional aspects of pain [6]. Signals transmitted during pain not only reach the somatosensory cortex for sensory interpretation but are also channeled to regions responsible for the emotional and affective aspects, notably the amygdala, hippocampus, and medial prefrontal cortex [7]. This limbic system involvement is essential for the experiential aspects of pain [8]. In the development of chronic pain, meanwhile glial cells, especially microglia play a role in pain processing by releasing neurotransmitters and inflammatory cytokines [9], the balance between the excitation and inhibition of neurons is critical for maintaining the normal function of the central nervous system [10]. Therefore, the inhibitory neuronal dysfunction in that corticolimbic system may contribute to the development, amplification, and perpetuation of the emotional-affective dimensions associated with chronic pain.

Parvalbumin (PV)-positive neurons are the largest subtype of γ-aminobutyric acid (GABA)-ergic interneurons and are distinguished by expression of the calcium-binding protein PV. They orchestrate the coordinated rhythmic activity of primary neurons via feed-forward inhibition, thus maintaining the balance between excitatory and inhibitory signals within the brain [11]. Accumulating evidence suggests that PV-positive neurons play a fundamental role in modulating brain activity to generate appropriate behavioral responses [12], while their functions are dysregulated under a variety of stressful conditions [13,14]. PV-positive neurons have been implicated in the development of hyperalgesia in mice experiencing fibromyalgia pain [15]. In addition, multiple pathologies, including Alzheimer's disease, schizophrenia, cognitive impairment, autism, melancholy, and other psychiatric disorders are also associated with PV-positive neurons [16]. However, the role of PV-positive neurons induced by neuropathic pain and emotional-affective dimensions remains unclear.

Cholecystokinin (CCK)-positive neurons in the central nervous system include pyramidal and basket cells. While PV-positive interneurons are known to inhibit the activity of excitatory pyramidal cells, CCK-positive interneurons can modulate the activity of other inhibitory neurons. This intricate interplay contributes to the regulation of network activity and is crucial for maintaining the balance between excitation and inhibition in the brain [17]. CCK has been reported to mediate the development and maintenance of hyperalgesia associated with peripheral neuropathy, particularly in pain that is exacerbated by anxiety [18]. In our previous studies, the density of CCK-positive neurons increased in certain subregions of the amygdala, hippocampus, and medial frontal cortex in rats with type 2 diabetes exhibiting anxiety-like behaviors although there was no difference in the proportion of these cell subtypes (regarding inhibitory-excitatory cells or cell sizes) [19–21]. Therefore, CCK-positive neurons may be specifically altered and associated with anxiety-like behaviors induced by pain.

Neuropathic pain is one of the main causes of chronic pain. However, modeling neuropathic pain in humans is complex because only stimuli that do not cause irreversible harm can be used. Therefore, animal models of peripheral nerve injury are needed to expand our understanding of the mechanisms underlying neuropathic pain-induced anxiety. Partial sciatic nerve ligation (pSNL), a neuropathic pain model, can present with pain symptoms for up to 7 months [22]. It is a moderate-symptom model of mechanical allodynia, heat-evoked hyperalgesia, and spontaneous pain that replicates some of the most prominent characteristics of clinical neuropathic pain [23]. Additionally, sex differences significantly influence the results of pain perception and behavioral tests in rats, often due to hormonal fluctuations during the menstrual cycle and postpartum period in females [24]. Consequently, to exclude the potential impact of these hormonal variations, this study employs the pSNL model in male rats.

The immediate-early gene, *c-Fos* has been widely acknowledged as a reliable marker for assessing neuronal activity, making it a significant resource for identifying cells activated in response to various stimuli [25,26]. The use of acute exposure to exploratory-based approach/-avoidance conflict tests is a methodological strategy used to identify specific brain areas involved in the generation of emotional reactions [27].

This study aims to investigate the time-dependent effect of neuropathic pain on the development of anxiety-like behaviors and whether this interaction is associated with PV- and CCK-positive neurons within the corticolimbic regions.

2. Methods

2.1. Animals

Eight-week-old male Wistar rats obtained from Japan SLC, Inc. (Shizuoka, Japan) were used for the experiments. We housed three rats per cage under a 12-hour light/dark cycle (lights on from 8:00 a.m. to 8:00 p.m.), with controlled temperature (22–24 °C) and humidity (70–80%). Rat chow and water were provided ad libitum. This study was approved by the Institutional Animal Care and Use Committee of Hiroshima University (A20–159) and performed according to the Hiroshima University Regulations for Animal Experimentation. All experiments were conducted in accordance with the National Institutes of Health Guidelines for the Care and Use of Laboratory Animals.

2.2. Neuropathic pain model and experimental design

pSNL was applied to the neuropathic pain model according to the method described by Seltzer et al. [22]. Briefly, after 7–10 days of acclimation to determine the baseline pain threshold, all rats were given deep anesthesia by intraperitoneal injection of a mixture of medetomidine (0.15 mg/kg), midazolam (2 mg/kg), and butorphanol (2.5 mg/kg). The left sciatic nerve was carefully freed from the surrounding connective tissue near the trochanter. Approximately one-third to one-half of the dorsum of the nerve was tightly ligated with 6–0 braided silk at a site just distal to the point at which the posterior biceps semitendinosus nerve branched off (pSNL rats) under a microscope. In the control group (sham rats), the sciatic nerve was exposed but left unaffected. After surgery, the nociceptive behavior was measured weekly, and anxiety-like behaviors were assessed biweekly. At 2 or 8 weeks after surgery, immediately after completing the behavioral test, the rats were humanely killed, and their brains were harvested for sampling (Fig. 1A).

2.3. Nociceptive behavior by von Frey test

The manual von Frey test was used to assess mechanical allodynia, a pain-like behavior. We measured the hind-paw withdrawal threshold once a day for 3 days before surgery (pre) and weekly after surgery. The rats were placed individually in testing chambers on wire mesh platforms (Ugo Basile SRL, Gemonio, Italy) and left undisturbed for 30 min to habituate them to the new environment. Each hind paw was tested for touch sensitivity by pricking filaments (Aesthesio® Precise Tactile Sensory Evaluator, DanMic Global, LLC, San Jose, CA, USA) perpendicular to the plantar surface until the filaments buckled slightly, and the filaments were held in that position for 5 s. Each filament was applied four more times at 60-second intervals. A response was

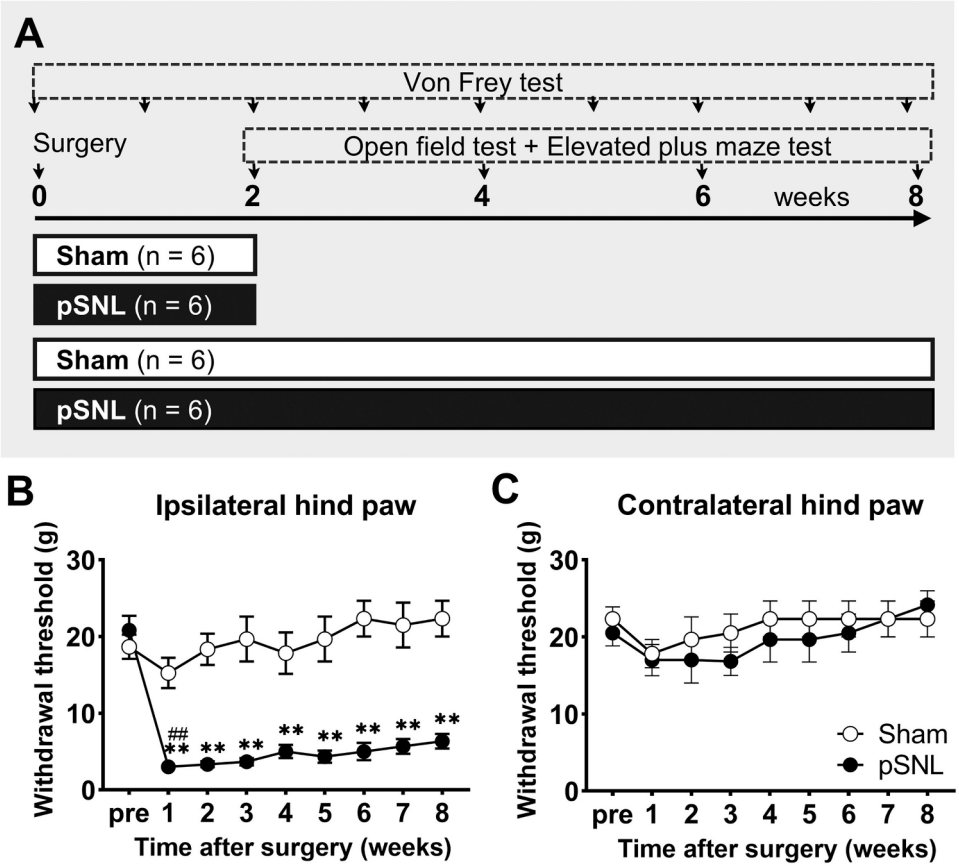

Fig. 1. Experimental design and nociceptive behaviors. (A) Eight-week-old male Wistar rats were acclimatized to laboratory conditions 7–10 days before surgery. During the operation of the left hind paw, rats were randomly divided into pSNL and sham groups (the sciatic nerve was exposed but not ligated). Pain threshold was measured once a day for 3 days before surgery and weekly after surgery using the manual von Frey test. Open field and elevated plus maze (EPM) tests were performed biweekly after surgery. At 2 or 8 weeks after surgery, immediately after completing the EPM test, rats were humanely killed, and brains were harvested for sampling. (B) Ligation led to mechanical allodynia, the withdrawal thresholds were reduced after surgery in the ipsilateral hind paw of pSNL rats compared with that of corresponding paw of sham rats and the pre-surgery threshold. (C) No difference was observed in the contralateral hind-paw parameters between groups. Data are presented as mean ± standard error of the mean. The differences were estimated by two-way repeated-measures analysis of variance with Bonferroni post hoc test: * *$p < 0.001$ (sham vs. pSNL), $^{\#\#}p < 0.001$ (post-surgery vs. pre-surgery). pSNL, partial sciatic nerve ligation; pre, before surgery.

considered positive if the animal exhibited nociceptive behaviors, including brisk paw withdrawal, licking, or shaking. Filaments were applied with forces of 1, 2, 4, 6, 8, 10, 15, and 26 g, the withdrawal thresholds of the hind paw were scored as a response using the "ascending stimulus" method (increasing monofilament force until positive response rates were >40% with the same filament) [28].

2.4. Anxiety-like behavior tests

Open field (OF) and elevated plus maze (EPM) tests were performed to assess anxiety-like behaviors during the dark phase (8–11 p.m.), as previously reported, with minor modifications [19,21]. The main goal was to pinpoint the specific time at which pSNL rats displayed emotional disorders, specifically anxiety disorders. The test-retest protocol was implemented with a 2-week interval after surgery, with a particular emphasis on discerning differences between the pSNL and sham groups. The EPM test was conducted the day after the OF test. Rats were transferred to the testing room in covered cages and acclimated for at least 30 min before testing. The sham and pSNL rats were tested alternately. All rats were given 10 min to freely explore the experimental fields, and their behavior was captured on video (PowerShot SX720 HS; Canon, Tokyo, Japan). After each test, the fields were cleaned with 70% ethanol to remove any odors.

In the OF test, the apparatus was a 90-cm-diameter circular black plastic sheet surrounded by a wall with a height of 70 cm. They were divided into a central area (central circular region, 45 cm in diameter) and a peripheral area. Illumination in the central area was 260 lx. The test was initiated by placing each animal at the center of the field. Locomotive behavior and time spent in different areas were analyzed using the AnimalTracker package (http://animaltracker.elte.hu [29]) of ImageJ (National Institute of Health, Bethesda, MD, USA); other behaviors, including rearing (frequency), grooming (duration), and inactivity (duration), were manually analyzed. Since the temporal exploration during behavioral tests can provide insights into the emotional states of rats [30]. It's observed that rats typically exhibit high levels of activity in the initial exploration phase. However, over time, they tend to habituate to the environment, resulting in a decrease in exploratory behavior [31,32]. A low activity level in the initial stage could be considered an indicator of anxiety or impaired adaptability to novel environments. We calculated the percentage of rearing in the center area using the formula 100 × [number of rearings in the center area] / [total number of rearings] and the percentage of rearing in the first 5 min of the 10-minute test using the formula 100 × [number of rearings in the first 5 min of the test] / [total number of rearings].

In the EPM test, the apparatus consisted of four arms (50 cm long and 10 cm wide) raised 60 cm above the floor. Two arms had walls (50 cm high; closed arms), whereas the remaining arms had no walls (open arms). The illumination was 315 lx at the ends of the open arms, 16 lx at the ends of the closed arms, and 230 lx at the intersecting area. In the preliminary experiments, rats exhibited less exploratory activity during

the initial period of the test when placed facing the open arms compared to when facing the closed arms. To obtain a more detailed evaluation of rat activity during the first few minutes the rats were positioned at the intersection facing the closed arm to begin the test. We analyzed the time spent, the frequency of movement along the arms, and the frequency of rearing in the separated arms. The durations of grooming and inactive conditions, as well as the latency to enter the open arms, were measured. The number of head dips over the edge was counted.

Some criteria of activities for both OF and EPM tests are as follows: rearing: rising on the hind limbs (HL), being in the arm: all four paws entering the arm, moving along the arms: walking or running completed an arm's distance, inactive condition: including immobility without sniffing or stretched attend posture.

2.5. Tissue preparation

Ninety minutes after the EPM test at 2 and 8 weeks after surgery, the rats were anesthetized with an overdose of sodium pentobarbital (100 mg/kg) and transcardially perfused with heparin saline solution and 4% paraformaldehyde in 0.1 M phosphate buffer (PB). The brains were removed, weighed, and stored in the same fixative for 24 h at 4 °C. Then, the brains were placed in 30% sucrose solution until they sank; they were then coronally sectioned at 30-μm thickness using a freezing microtome (REM-710 + Electro Freeze MC-802 C; Yamato Kohki, Saitama, Japan). Six serial sets of free-floating sections were collected in 24-well plates filled with phosphate-buffered saline (PBS) 0.01 M until sectioning was completed. All sets were anatomically similar to the others. The sections were transferred to a cryoprotectant solution (glycerol/ethylene glycol/PBS, 3:3:4) and stored at − 30 °C until processing.

2.6. Immunohistochemistry

For immunohistochemistry, we used a standard avidin–biotin procedure using a free-floating method. First, the sections were brought to room temperature for 30 min and then washed in PBS 0.01 M. Those sections were quenched endogenous peroxidases in 2% hydrogen peroxide (H_2O_2) and 20% methanol for 10 min. Following the sections were washed in PBS containing 0.25% Triton X-100 (PBS-T) and blocked with 3% normal horse serum for 30 min. After washing in PBS-T, the sections were incubated with one of the primary antibodies: rabbit anti-PV (1:10,000; Sigma, St. Louis, MO, USA), rabbit anti-CCK (1:10,000, Sigma) or mouse anti-*c-Fos* (1:1000; Abcam, Cambridge, UK) in 1% blocking solution at 4 °C. The next day, after 16 h of incubation, the sections were washed in PBS-T and incubated on ice for 1 h with secondary antibodies at a 1:500 dilution of biotinylated anti-rabbit (for PV and CCK staining) or biotinylated anti-mouse (for *c-Fos* staining; Vector Laboratories, Burlingame, CA, USA). After washing in PBS-T, the sections were incubated with an avidin–biotin–peroxidase complex (1:200; ABC-Elite, Vector Laboratories) for 1 h, washed in PBS, and visualized using 0.03% H_2O_2 and 0.025% diaminobenzidine (Dojindo Laboratories, Kumamoto, Japan). Finally, the sections were mounted on gelatinized glass slides, air-dried, dehydrated in ascending alcohol, cleared in xylene, and coverslipped using Entellan New (Merck, Darmstadt, Germany).

2.7. Immunofluorescence

For immunofluorescence analysis, free-floating sections were rinsed with PBS or PBS-T between each incubation step. After blocking with 3% normal goat serum for 30 min at room temperature, the sections were incubated simultaneously with rabbit anti-PV (1:5000; Sigma) and mouse anti-*c-Fos* (1:500; Abcam) in PBS-T containing 1% goat serum overnight at 4 °C. The sections were then incubated sequentially for 1 h at room temperature with the conjugated fluorochrome secondary antibodies Alexa Fluor 488 goat anti-rabbit (1:500; Cell Signaling Technology, Danvers, MA, USA) and Alexa Fluor 555 goat anti-mouse (1:200; Cell Signaling Technology). To improve the positive signal contrast by reducing nonspecific background noise, an autofluorescence quencher (Vector Laboratories) was used to incubate the sections for 5 min. Finally, the sections were mounted on methylated albumin silane-coated glass slides and coverslipped using 4′,6-diamino-2-phenylindole (DAPI; Vector Laboratories) for nuclei staining. For all staining procedures, negative control sections were processed identically, except for the omission of each primary antibody. No reaction products were observed in any of the control samples.

2.8. Measurements of cortical thicknesses and brain region area

Images were obtained using a light microscope (BX51; Olympus, Tokyo, Japan) and digitized with a camera (DP70; Olympus) for immunohistochemical staining of the sections with an appropriate objective lens. The images were analyzed using ImageJ. Data were collected from both hemispheres and averaged. Brain region landmarks were identified by examining anatomically matched adjacent Nissl-stained sections in reference to the Paxinos and Watson rat brain atlas [33]. We measured the sensory cortical thickness in three sections: anterior to posterior (AP), 2.28, − 1.80, and − 5.20 mm from the bregma, based on a previous study [34]. These measurements included four lines on one side: the medial elevation line of the corpus callosum and three additional lines 1 mm lateral to the medial measurement line. Values from the four lines were averaged for each AP level. The following brain regions were used for measuring the area and analyzing cells: the amygdala, including the central amygdala (CeA), medial amygdala (MeA), and basolateral amygdaloid complex (BLC) constisting of lateral amygdala (LA) and basolateral amygdala (BLA) nuclei at AP − 2.10, − 2.28, − 2.46, and − 2.64 mm; hippocampus, including hippocampal cornu ammonis (CA) areas 1, 2, and 3 and the dentate gyrus (DG) at AP − 2.76, − 2.94, and − 3.12 mm; the medial prefrontal cortex (mPFC), including the prelimbic cortex (PL), infralimbic cortex (IL), and anterior cingulate cortex (ACC) at AP + 3.12, + 2.94, and + 2.76 mm; primary somatosensory cortex (S1), including the forelimb (FL) and HL at AP − 0.84, − 1.12, and − 1.20 mm; and insular cortex, including granular insula (GI), dysgranular insula (DI), and agranular insula (AI) AP at − 0.12, − 0.30, and − 0.48 mm from the bregma.

2.9. Cell analysis

The analysis of c-Fos, PV, and CCK-positive neurons was conducted in rats at both 2 and 8 weeks after surgery. For *c-Fos*-positive neuron counting, brain sections were first examined using dark-field microscopy to determine the structures of interest, and a series of 20 × magnification images (0.1343 mm^2/image) were acquired for every subregion in all sections (2–5 images per subregion). *C-Fos* staining was quantified using the same acquisition settings as in ImageJ. After converting these images into black-and-white 256 gray-level images, a 62% background threshold (quotient between the intensity of the background label and the intensity of the core label) and the size of the object were set. Pixels within this range were converted to black, and those outside this range were converted to white. The threshold was determined to obtain clear objects representing the *c-Fos*-labeled nuclei. The Analyze Particles package in ImageJ was used to automatically count all cell profiles after setting the object area threshold (25–200 μm^2) and shape (0.3–1). The neuronal density (neurons/mm^2) was estimated.

For CCK- and PV-positive neuron counting, larger magnified acquired images were used to count neuron somatic profiles by manually clicking the Cell Counter (written by Kurt De Vos; https://imagej.nih.gov/ij/plugins/cell-counter.html) plug-in for ImageJ. Neurons with detectable CCK and PV immunoreactivity above the background level were selected as CCK- or PV-positive neurons. No signals from the vessels, blood cells, or reaction precipitates were counted.

Since morphological differences in PV-positive neurons may correspond to functional differences [35], the somata size and intensity of all PV-positive neurons in the regions of interest were measured using ImageJ software with the freehand selection method. The classification of PV-positive neurons into large or small cells was based on previous studies [36,37].

To identify PV-positive neurons coexpressing *c-Fos*, two or three representative fluorescently labeled sections from each region were examined using a confocal laser scanning microscope (STELLARIS 5; Leica Microsystems, Wetzlar, Germany). Confocal images (size, 581.25 × 581.25 μm) were taken with a 20 × dry objective lens in Z-stacks, 1 μm thick at a resolution of 1024 × 1024 and speed of 400 Hz. Quantitative evaluations were performed using the LAS X Office version 1.4.4 (Leica Microsystems), which allows the simultaneous navigation of a positive signal in the merged image and single-channel images at the z-stack level. The cell numbers of single-labeled neurons were counted in one channel, and the colocalized cells were counted in the merged channels. Only PV- or *c-Fos* immunofluorescence-positive neurons with DAPI were counted. The examination of cell densities was conducted on both hemispheres and the outcomes were combined into an average.

2.10. Statistical analysis

Data are expressed as mean ± standard error of the mean. All statistical analyses were performed using SPSS version 19.0 (IBM Japan, Tokyo, Japan). Shapiro—Wilk and Levene's tests were used to assess the normality and homogeneity of variance, respectively. A 4 × 2 analysis of variance (ANOVA) with the within-subject factor testing time (*2, 4, 6, 8 weeks after surgery*) and between-subject factor group (*sham, pSNL*) was performed for behavioral parameters. A 2 × 2 ANOVA with the between-subject factors testing time (*2, 8 weeks after surgery*) and group (*sham, pSNL*) was performed for the morphological parameters. Simple Effects Tests with Bonferroni adjustment was performed if any ANOVA indicated a significant in the main effect of group or interaction between group and time. Kolmogorov–Smirnov tests were used to assess disparities in the distribution of the PV-positive somata area between groups using cells as statistical units. Mann—Whitney U test was performed for the percentage of large PV-positive neurons and results of double staining. Correlations were evaluated using Spearman's rank correlation coefficient. Statistical analyses were performed using IBM SPSS Statistics, version 19.0 (IBM Corp., Armonk, N.Y., USA). The significance level was set at $\alpha = 0.05$, or $\alpha = 0.017$ (Bonferroni adjusted for multiple correlations).

3. Results

3.1. Nociceptive behaviors in neuropathic rats

Plantar tests were performed to assess the effects of pSNL on mechanical allodynia. Following ligation surgery, the hind-paw withdrawal threshold significant decreased compared with preoperative threshold or that of sham-operated rats. The pSNL rats displayed consistently reduced mechanical withdrawal thresholds in the ipsilateral hind paw at all testing time points, indicating mechanical allodynia [$F(1,10) = 211.51$, $p < 0.001$] (Fig. 1B). However, no significant differences in these thresholds in the contralateral hind paw were observed over time between the groups [$F(1,10) = 1.51$, $p = 0.245$] (Fig. 1C). All animals had regular body weight development throughout the study period.

3.2. Emotional behaviors in neuropathic rats

We conducted OF and EPM tests to examine the influence of nerve injury or pain on anxiety-like behaviors. Spontaneous locomotor activity was quantified and categorized into inactive conditions, grooming activities, and general exploration activities, both horizontally and vertically. Some behaviors were evaluated in terms of their temporal aspects [38].

During the OF tests, behavior was evaluated in distinct areas, including the central and peripheral areas. At 4 and 6 weeks after surgery, pSNL rats spent less time in the center of the field than sham rats with adjusted-p value = 0.049 and 0.019, respectively, following a significant main effect of group [$F(1,10) = 11.81$, $p = 0.003$] (Fig. 2A). There were no significant differences between the groups in the total distance traveled or the total number of rearings throughout the experimental period (Table 1). However, from 4 weeks after surgery, pSNL rats exhibited fewer rearings in the central area than sham rats (Fig. 2B) with a significant main effect of group [$F(1,10) = 11.22$, $p = 0.007$] and a significant interaction between group and time [$F(3,30) = 5.73$, $p = 0.003$]. Sham rats showed high levels of rearing at the beginning of each OF test, whereas the pSNL rats exhibited a decreased rearing activity in the first 5 min of the 10-minute test with a significant main effect of group [$F(1,10) = 32.02$, $p < 0.001$] and a significant interaction between group and time [$F(3,30) = 3.66$, $p = 0.023$]. These significant differences were observed at 4, 6, and 8 but not at 2 weeks after surgery (Fig. 2C). Additionally, 6 weeks after surgery, the distance traveled in the center area by pSNL rats was lower than that of the corresponding parameters in sham rats with adjusted-p = 0.019 following a significant main effect of group [$F(1,10) = 5.79$, $p = 0.036$] (Table 1) The inactivity time and grooming time was comparable between the groups regardless of time assessment (Table 1).

During the EPM test, behavioral parameters were assessed in different divisions, including the open and closed arms. At 4, 6, and 8 weeks after surgery, the pSNL group exhibited reduced exploratory activities in the open arms compared with the sham group (Fig. 2D, E, F, G). From 4 weeks after surgery, pSNL rats spent less time in the open arms with a significant main effect of group [$F(1,10) = 43.32$, $p < 0.001$] and a significant interaction between group and time [$F(3,30) = 4.93$, $p = 0.007$] (Fig. 2D). pSNL rats also less engaged in walking or running in the open arms with a main effect of group [$F(1,10) = 15.51$, $p = 0.003$] (adjusted-p = 0.041; < 0.001 and 0.045 for pairwise comparisons between groups at 4; 6 and 8 weeks after surgery, respectively), but there was no significant interaction between group and time (Fig. 2E). Meanwhile, the total movement along the arms in both open and closed arms was similar in the pSNL rats compared to the sham rats (Table 2). The percentage of rearing in the open arms and intersection area decreased in the pSNL group compared with the sham group with adjusted-p values < 0.001 at 4; 6 or 8 weeks after surgery; there was a significant main effect of group [$F(1,10) = 87.0$, $p < 0.001$] and a significant interaction between group and time [$F(3,30) = 22.97$, $p < 0.001$] (Fig. 2F). Moreover, the pSNL group exhibited an anxious condition in the open arms, as indicated by significant reduced head-dipping from 4 weeks after surgery with a significant main effect of group [$F(1,10) = 28.39$, $p < 0.001$] and a significant interaction between group and time [$F(3,30) = 3.23$, $p = 0.03$] (Fig. 2G). Although significant differences among the groups were observed only at 4 weeks after surgery (adjusted-p < 0.05), the pSNL rats showed a longer latency to enter the open arms at other assessed time points with a main effect of group [$F(1,10) = 5.34$, $p = 0.043$] (Table 2). Additionally, 8 weeks after surgery, the pSNL rats exhibited a decrease in the total number of rearings, which represents vertical exploration activity (adjusted-p = 0.002, following interaction between group and time [$F(3,30) = 5.38$, $p = 0.004$]; Fig. 2H), and a significant increase in inactive duration (adjusted-p < 0.001 following a main effect of group [$F(1,10) = 24.80$, $p < 0.001$] and interaction between group and time [$F(3,30) = 3.86$, $p = 0.019$]; Fig. 2I).

These results suggest that pSNL rats exhibit anxiety-like behaviors from 4 weeks after surgery, but not at 2 weeks. It is noteworthy that a decreased vertical activity and an increased inactive behavior were observed in the pSNL group 8 weeks after surgery.

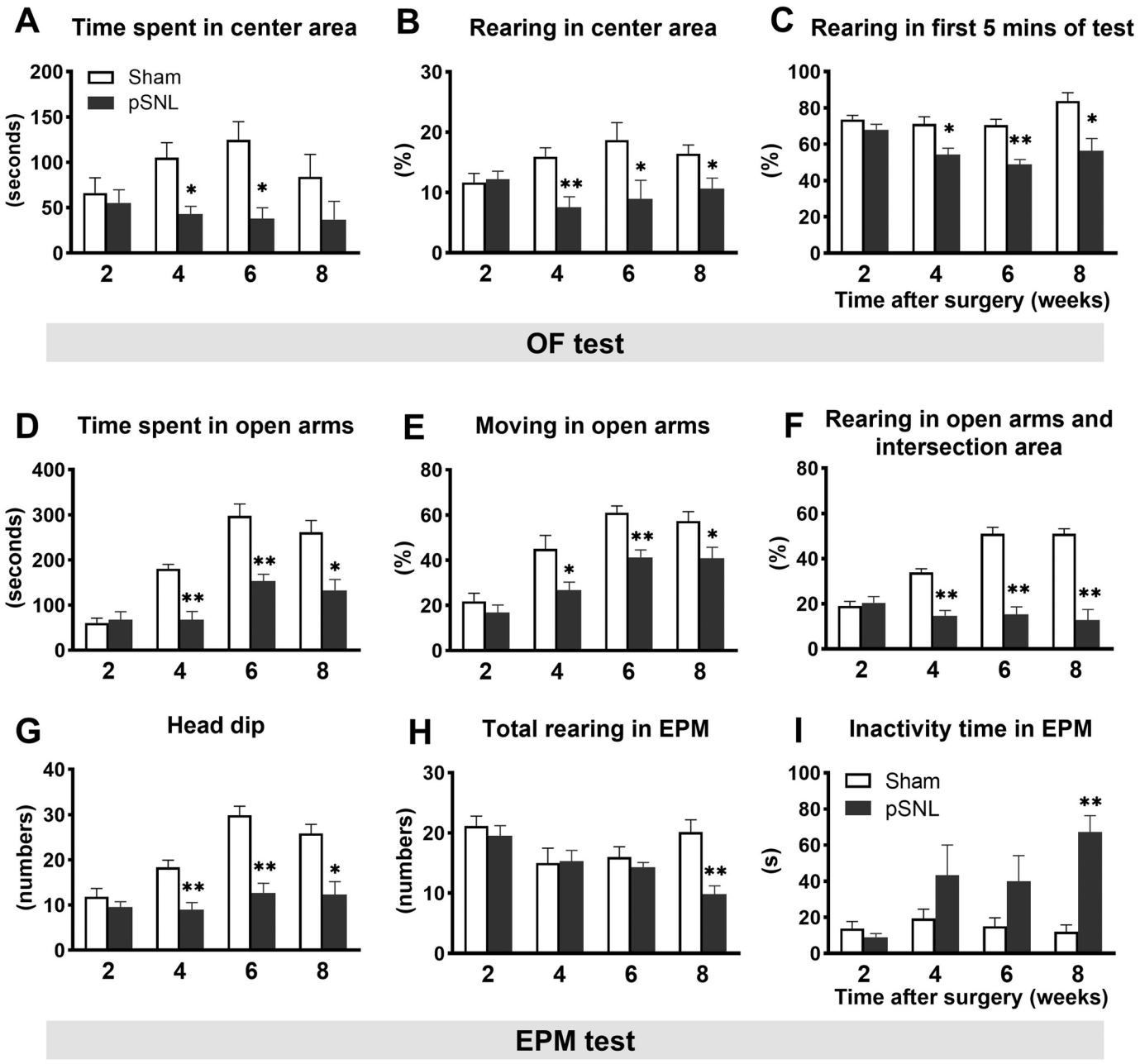

Fig. 2. Behavioral parameters in the open field and elevated plus maze tests. (A) Time spent in center area, (B) percentages of rearings in the center area, and (C) percentages of rearings in the first5 minutes of the 10-minute test in open field (OF). (D) Time spent in the open arms, (E) percentages of moving in the open arms, (F) percentages of rearing in the open arms and intersection area, (G) number of head dips, (H) total number of rearings, and (I) total inactivity time in the elevated plus maze (EPM). Data are presented as mean ± standard error of the mean. *Significant difference from the sham group: *$p < 0.05$, * *$p < 0.001$, two-way repeated-measures analysis of variance followed by Bonferroni post hoc test. pSNL, partial sciatic nerve ligation.

3.3. Brain weights and subregional areas

To investigate the neuroanatomical mechanisms underlying the altered anxiety-like behaviors in pSNL rats, we assessed several parameters, including body and brain weight, somatosensory cortical thickness, and area of the corticolimbic system. When comparing different time points after surgery, all these parameters were significantly higher in 8-week post-surgery rats than in 2-week post-surgery rats ($p < 0.001$). However, we did not observe any significant differences in the sizes of these brain structures between the pSNL and sham groups, regardless of the time after surgery (Supplemental Fig. 1).

3.4. Density of c-Fos-, PV- and CCK-positive neurons

To explore the mechanisms underlying the altered emotional behavior in pSNL rats, we measured the densities of *c-Fos*-, PV-, and CCK-positive neurons in specific corticolimbic regions related to pain processing, including the amygdala, hippocampus, mPFC, S1 primary somatosensory cortex, and insular cortex at both 2 and 8 weeks after surgery.

To identify the brain regions that correlate with the anxiety phenotype, all animals underwent an EPM test and were humanely killed after 90 min. *c-Fos* expression was also evaluated (Fig. 3). Two-way ANOVA [time (2) × group (2)] revealed significant simple main effect of group in the CeA [$F(1,20) = 5.63$, $p = 0.028$), LA [$F(1,20) = 15.83$,

Table 1
Behavioral parameters in the open field test.

	2w		4w		6w		8w	
	Sham	pSNL	Sham	pSNL	Sham	pSNL	Sham	pSNL
Total distance traveled (m)	21.7	30.8	20.6	22.6	20.7	17.7	14.4	17.9
	(1.9)	(2.7)	(2.3)	(2.7)	(2.4)	(4.4)	(2.7)	(2.8)
Distance traveled in the center area (m)	3.6	2.9	3.6	2.2	5.1	1.8 * (0.8)	2.2	1.6
	(0.9)	(0.8)	(1.0)	(0.4)	(0.8)		(0.8)	(0.8)
Total rearing in OF (numbers)	17.7	19.2	25.2	14.3	23.8	13.8	15.3	15.5
	(0.9)	(4.1)	(3.7)	(2.6)	(3.3)	(2.1)	(2.9)	(2.2)
Grooming time in OF (s)	55	55	52	56	36	55	30	45
	(18)	(15)	(20)	(19)	(23)	(25)	(7)	(11)
Inactivity time in OF (s)	110	89	78	130	125	148	132	143
	(34)	(37)	(19)	(27)	(35)	(33)	(37)	(37)

Values represent the mean (standard error of means).
*Significant difference from the sham group, $p < 0.05$, two-way repeated-measures ANOVA followed by Bonferroni post hoc test.

Table 2
Behavioral parameters in the elevated plus maze test.

	2w		4w		6w		8w	
	Sham	pSNL	Sham	pSNL	Sham	pSNL	Sham	pSNL
Total moving along the arms (numbers)	38.3	40.3	46.3	38.3	42.7	43.3	39.5	38.7
	(6.0)	(4.2)	(4.8)	(4.3)	(4.3)	(3.6)	(3.6)	(3.5)
Grooming time in EPM (s)	25	27	11	11	7	27 *	8	23
	(3)	(6)	(4)	(5)	(1)	(6)	(3)	(9)
Latency to enter the open arms (s)	195	220	84	206 *	47	87	33	53
	(69)	(69)	(14)	(14)	(16)	(16)	(8)	(38)

Values represent the mean (standard error of means).
*Significant difference from the sham group, $p < 0.05$, two-way repeated-measures ANOVA followed by Bonferroni post hoc test.

$p = 0.001$], BLA [$F(1,20) = 36.09$, $p < 0.001$], CA1 [$F(1,20) = 46.49$, $p < 0.001$], and CA2 [$F(1,20) = 71.13$, $p < 0.001$]. There were significant interactions between group and time in the BLA [$F(1,20) = 5.71$, $p = 0.027$], CA1 [$F(1,20) = 19.81$, $p < 0.001$], and CA2 [$F(1,20) = 29.31$, $p < 0.001$]. Using Bonferroni post hoc test analysis for 2-week post-surgery animals, we found that the density of *c-Fos*-positive cells in the CeA was higher in pSNL rats than in sham rats ($p < 0.001$) meanwhile this parameter in the remaining examined brain regions was not significantly different between the groups (Fig. 3E). Eight weeks after surgery, *c-Fos* expression in the pSNL group increased significantly in the LA ($p < 0.001$), BLA ($p = 0.012$), and CeA ($p < 0.001$) subfields of the amygdala as well as in the CA1 ($p < 0.001$) and CA2 ($p < 0.001$) subfields of the hippocampus compared with the sham group (Fig. 3E). No significant differences in *c-Fos* expression were observed in the remaining subregions between the sham and pSNL groups or among the different time points after surgery (Supplemental Fig. 3 A).

To investigate the role of inhibitory circuits in emotion and pain processing, we analyzed the expression of PV-positive neurons (Fig. 4). Within the amygdala, PV-positive neurons were primarily found in the basolateral amygdaloid complex, whereas a few were observed in the MeA or CeA (Fig. 4A, B). Eight weeks after surgery, the densities of PV-positive neurons in the LA and BLA were significantly lower in pSNL rats than in sham rats. The analysis showed a significant main effect of group in LA [$F(1,20) = 21.19$, $p < 0.001$] and BLA [$F(1,20) = 10.03$, $p = 0.005$]. There were significant interactions between group and time [LA: $F(1,20) = 52.99$, $p < 0.001$; BLA: $F(1,20) = 31.26$, $p < 0.001$], and a significant simple main effect at 8 weeks after surgery, with an adjusted p-value < 0.001 in both the LA and BLA subregions. In the hippocampal area, increased PV expression was observed in the CA1 ($p < 0.001$) and CA2 ($p < 0.001$) subregions of the pSNL group compared with the sham group at 8 weeks after surgery. There were significant interactions between group and time for the CA1 [$F(1,20) = 21.09$, $p < 0.001$] and CA2 [$F(1,20) = 73.20$, $p < 0.001$]. However, no significant difference in PV expression was observed between sham and pSNL rats in the CA3 and DG subregions, regardless of the time after surgery. In the S1 primary somatosensory cortex, we observed a significant main effect of group in the density of PV-positive neurons in the HL and FL subregions with $F(1,20) = 39.29$, $p < 0.001$ and $F(1,20) = 6.69$, $p = 0.016$, respectively. There were significant interactions between group and time in the FL [$F(1,20) = 4.75$, $p = 0.041$] but not in the HL [$F(1,20) = 1.66$, $p = 0.212$]. The Bonferroni post hoc test revealed that the density of PV-positive neurons in the HL of the pSNL group was significantly higher than that of the sham group at both 2 ($p = 0.002$) and 8 weeks after surgery ($p < 0.001$). Similar patterns were observed in the FL subregion, but only at 8 weeks after surgery, with an adjusted p-value of 0.003.

CCK expression was significantly higher in the density of CCK-positive neurons in pSNL rats than in sham rats within the LA and BLA subregions 8 weeks after surgery (Supplemental Fig. 2). As shown in Fig. 5, there were significant main effects of group in the LA [$F(1,20) = 5.39$, $p = 0.031$] and the BLA [$F(1,20) = 13.53$, $p = 0.001$], and a significant interaction between group and time in the BLA [$F(1,20) = 10.08$, $p = 0.005$]. We also observed significant effects of time in the BLA [$F(1,20) = 10.08$, $p = 0.005$], CA1 [$F(1,20) = 9.46$, $p = 0.006$], CA2 [$F(1,20) = 29.24$, $p < 0.001$], and FL [$F(1,20) = 58.75$, $p < 0.001$] subregions. CCK-positive neurons were not detected in the CeA and MeA. The densities of CCK-positive neurons in the other brain subregions evaluated were comparable between the groups at both 2 and 8 weeks after surgery.

In the mPFC and insular cortex regions, no significant difference in *c-Fos*, PV, or CCK expression was found between sham and pSNL rats (Supplemental Fig. 3).

3.5. Relationships between pain-like behavior, emotional behavior and histological alterations

The correlation between paw withdrawal threshold and time spent in open arms in the EPM test aimed to assess the link between pain-like and anxiety-like behaviors. Spearman's rank test showed a significant positive correlation at 4-, 6-, and 8-week post-surgery ($p = 0.028$, < 0.001, 0.019). However, no relationship between pain and anxiety behaviors was noted at 2 weeks after surgery ($p = 0.872$).

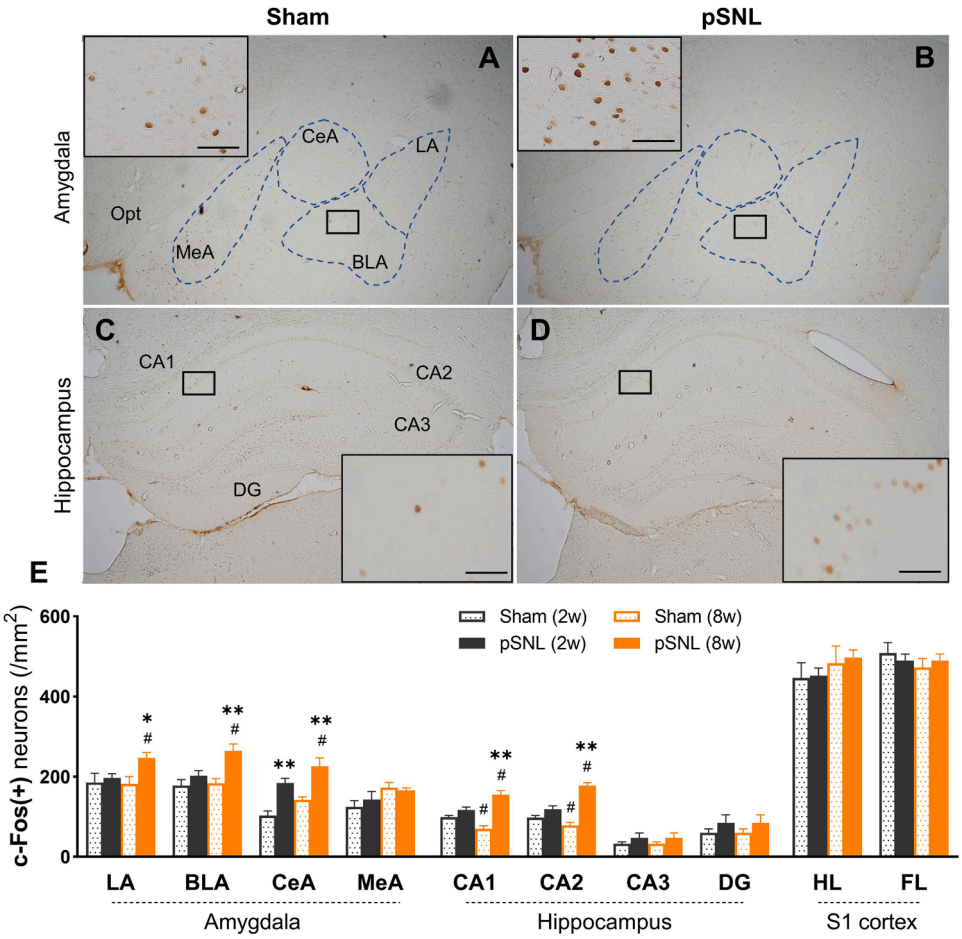

Fig. 3. . c-Fos-positive neurons. Photomicrographs illustrate c-Fos expression in the amygdala (A, B) and hippocampus (C, D) 8 weeks after surgery in rats. The example frames are shown at greater magnification (5 ×), scale bar = 50 μm. (E) Density of c-Fos-positive neurons. Data are presented as mean ± standard error of the mean. The differences were estimated by two-way analysis of variance with Bonferroni post hoc test: *$p < 0.05$ and * *$p < 0.001$ (sham vs. pSNL), $^{\#}p < 0.05$ (between times after surgery). pSNL, partial sciatic nerve ligation; LA, lateral amygdala; BLA, basolateral amygdala; CeA, central amygdala; MeA, medial amygdala; Opt, optic tract; CA1–3, cornu ammonis areas 1–3; DG, dentate gyrus; primary somatosensory (S1) cortex; HL, hind limb; FL, forelimb.

To explore the association between the densities of PV- or CCK-positive neurons and *c-Fos*-positive neurons, we conducted multiple correlation analyses (Table 3). We found a significant negative correlation between the density of PV-positive neurons and that of *c-Fos*-positive neurons in the BLA, whereas a significant positive correlation was observed in the CA2 subregion using a Bonferroni-adjusted α level of 0.017 (0.05/3). However, no significant correlation was observed between the density of CCK-positive neurons and that of *c-Fos*-positive neurons in these subfields.

Since significant correlations between pain-like behaviors and morphological changes (densities of PV- and c-Fos-positive neurons) were identified in the LA, BLA, CA1, and CA2 subregions at 8- but not at 2-week post-surgery (Supplemental Table 1). We further performed correlation analyses between anxiety-like behavioral parameters and the densities of *c-Fos*-, PV-, or CCK-positive neurons in all animals 8 weeks after surgery (Table 4). We found a significant negative correlation between the density of *c-Fos*-positive neurons and the time spent in the open arms during the EPM test in the LA, BLA, CA1, and CA2 subregions. The density of PV-positive neurons showed a significant negative correlation with the time spent in the open arms and those in the LA and BLA subregions, whereas a significant positive correlation was observed with those in the CA1 and CA2 subregions. However, no significant relationships were found between the density of CCK-positive neurons and the any behavioral parameters.

3.6. *Somata size and intensity of PV-positive neurons*

Alterations in PV-positive neurons in specific corticolimbic subregions were associated with anxiety-like behaviors in pSNL rats 8 weeks after surgery. Given the diverse subpopulations of PV-positive neurons based on their morphology, including cell size and intensity, we measured the somata size and average intensity of all PV-positive neurons (Fig. 6A) in the LA, BLA, CA1, and CA2 subregions. Kolmogorov–Smirnov tests were used to assess the distributional differences in these parameters between the sham and pSNL groups. Although no significant difference in PV-positive neuron intensity was observed, we found a leftward shift in the distribution of PV-positive somata size in the LA ($p < 0.001$) and BLA ($p < 0.001$) and a rightward shift in the CA1 ($p < 0.001$) of pSNL rats compared with the sham group at 8 weeks after surgery (Fig. 6B, C).

Considering the decrease in the density of PV-positive neurons in the amygdala subregions and the increase in CA1, we hypothesized that these alterations mainly occurred in cells with large somata. To validate this hypothesis, we classified PV-positive neurons into large and small subtypes using a cutoff value of 120 μm^2 based on previous studies [36, 37]. Eight weeks after surgery, the percentage of large PV-positive neurons was significantly reduced in the LA and BLA in the pSNL group compared with that in the sham group, with p-values of 0.004 and 0.015, respectively (Mann—Whitney U test; Fig. 6D). Additionally, we found a positive relationship between the percentage of large

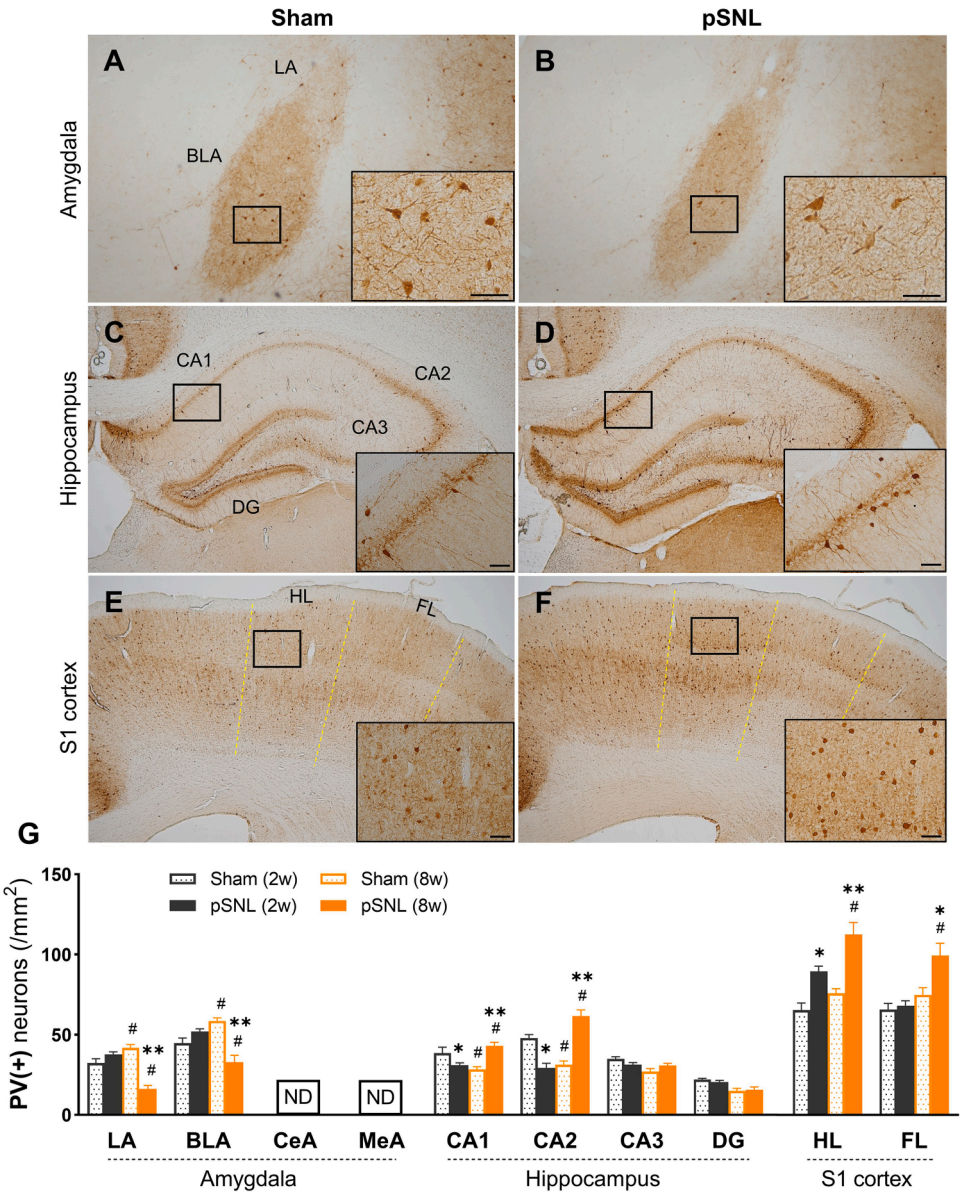

Fig. 4. PV-positive neurons. Photomicrographs illustrate PV expression in the amygdala (A, B), hippocampus (C, D), and S1 primary somatosensory cortex (E, F) area 8 weeks after surgery in rats. The example frames are shown at greater magnification, scale bar = 50 μm. (G) Density of PV-positive neurons. Data are presented as mean ± standard error of the mean. The differences were estimated by two-way analysis of variance with Bonferroni post hoc test: *$p < 0.05$ and * *$p < 0.001$ (sham vs. pSNL), $^{\#}p < 0.05$ (between times after surgery). PV, parvalbumin; pSNL, partial sciatic nerve ligation; LA, lateral amygdala; BLA, basolateral amygdala; CeA, central amygdala; MeA, medial amygdala; CA1–3, cornu ammonis areas 1–3; DG, dentate gyrus; HL, hind limb; FL, forelimb; ND, not detected.

PV-positive neurons in the LA and the total number of rearings in the EPM test and a negative relationship between the percentage of large PV-positive neurons in the BLA and the inactivity time in the EPM test (Fig. 6E, F).

3.7. Coexpression of PV and c-Fos in the amygdala

Eight weeks after pSNL, specific morphological alterations associated with pain-induced anxiety-like behaviors were observed in PV-positive neurons in the LA and BLA. To further investigate the activation characteristics of PV-positive neurons in the basolateral amygdaloid complex, we performed immunofluorescence co-staining with *c-Fos*. In the BLA, among the PV-positive neurons (Fig. 7C, G, J), the percentages of neurons coexpressing PV and *c-Fos* were 19.6% ± 3.7% in pSNL rats and 36.4% ± 6.4% in sham rats ($p = 0.002$, Mann—Whitney U test). Among the *c-Fos*-positive neurons (Fig. 7B, F, I), the percentages of PV expression were 1.9% ± 0.7% in pSNL rats and 10.3% ± 1.6% in sham rats ($p = 0.002$, Mann—Whitney U test). These PV-positive neurons showed varying activity levels when exposed to anxious conditions.

4. Discussion

Our primary findings indicate that pain induced by pSNL alters the emotionality of rats based on the progression of pain over time. Changes in the density of PV-positive neurons in the amygdala and hippocampal subregions are associated with anxiety-like behavior. Other altered characteristics of PV-positive neurons in the amygdala, including somata size and activated cell conditions may also be related to these behavior changes in pSNL rats.

In the present study, anxiety-like behavior of late phase, which was linked to paw withdrawal thresholds of neuropathic pain rats, could be found to be correlated with the densities of PV-positive neurons in

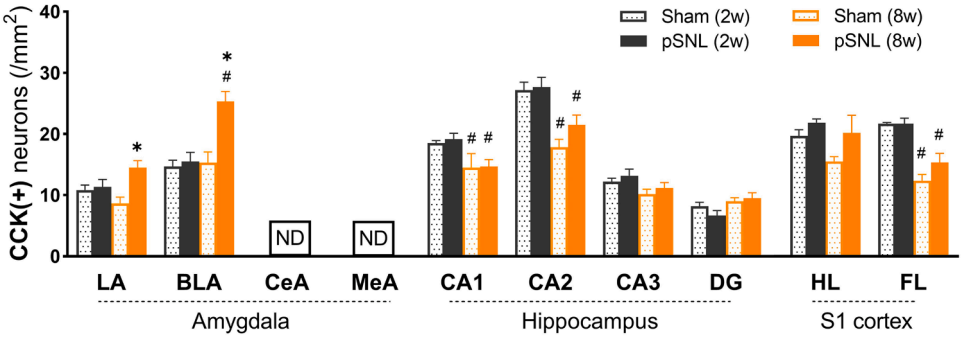

Fig. 5. Density of CCK-positive neurons. CCK, cholecystokinin; pSNL, partial sciatic nerve ligation; LA, lateral amygdala; BLA, basolateral amygdala; CeA, central amygdala; MeA, medial amygdala; CA1–3, cornu ammonis areas 1–3; DG, dentate gyrus; HL, hind limb; FL, forelimb; ND, not detected. Data are presented as mean ± standard error of the mean. The differences were estimated by two-way analysis of variance with Bonferroni post hoc test: *$p < 0.05$ (sham vs. pSNL), $^{\#}p < 0.05$ ($^{\#}$between times after surgery).

Table 3
Correlation matrix of c-Fos-, PV-, and CCK-positive neuron density in subregions at 8 weeks after surgery.

	LA			**BLA**	
	c-Fos (+)	PV (+)		c-Fos (+)	PV (+)
PV (+)	-0.60		PV (+)	-0.69 *	
	0.039			*0.012*	
CCK (+)	0.55	-0.43	CCK (+)	0.55	-0.66
	0.064	*0.159*		*0.056*	*0.019*
	CA1			**CA2**	
	c-Fos (+)	PV (+)		c-Fos (+)	PV (+)
PV (+)	0.66		PV (+)	0.88 *	
	0.02			*< 0.001*	
CCK (+)	-0.12	0.26	CCK (+)	0.49	0.52
	0.702	*0.417*		*0.110*	*0.081*

Data represents Spearman's rank correlation coefficient (upper) and p-value (lower).
PV, parvalbumin; CCK, cholecystokinin; LA, lateral amygdala; BLA, basolateral amygdala; CA1, cornu ammonis area 1; CA2, cornu ammonis area 2.
*Significant at the Bonferroni adjusted α level of 0.017 (0.05/3).

specific brain areas. By comparing to the sham group at the early and the late phase of pain, the PV-positive neuron density of pSNL rats in the HL subregion of the S1 primary somatosensory cortex increased at both time points examined, whereas it decreased in the amygdala subregions and increased in the hippocampal subregions at the late phase. These results suggested that the effect of pain on PV-positive cells varied and differed among distinct regions. Meanwhile, the density of PV-positive neurons remained unchanged with aging in numerous cortical areas of healthy mice [39], while prolonged stress resulted in PV alterations in subcortical regions [13]. The persistent and prolonged pain stimulus caused by sciatic nerve ligation induces significant structural and functional changes in the limbic–cortical circuitry [6]. Therefore, the observed changes in PV-positive neurons in rats are likely the result of persistent and severe stress induced by prolonged pain. As the S1 primary somatosensory cortex specializes in the perception and processing of nociceptive signals, its subregional plasticity has been reported to be altered in both acute and chronic pain [10,15,40]. The subregions of amygdala and hippocampus are responsible for the reception and integration of multidimensional painful stimuli [7,41]. Interestingly, correlations were found between the PV-positive neuron densities in the amygdala and hippocampal subregions and the anxiety-like behavioral parameters. Such associations indicate a potential mediating role of PV expression in the anxiety-like behaviors exhibited by pSNL rats. In addition, chemogenetic inhibition of PV-positive neurons in the BLA in mice have produced anxiogenic effects [42] and a moderate decrease in the density of PV-positive neurons in the BLA has been associated with a shorter time spent in the center zone of the OF test in *dt*^{sz} mutant hamsters [43]. Conversely, augmentation of PV-positive neuron density in the BLA has been linked to decreased anxiety-like behavior in rats housed under normal conditions [37]. These findings provide additional support for the hypothesis that PV-positive neurons in the amygdala and hippocampal subregions are involved in the anxiety-like behaviors induced by chronic neuropathic pain.

We found that the alteration in PV-positive neurons occurred primarily within large cell subtypes in rats with pain-induced anxiety-like behaviors. PV-positive neurons exhibit considerable heterogeneity in subpopulations with distinct soma characteristics. In the context of the basolateral amygdaloid complex, our results revealed a correlation between the reduction in large PV-positive cells and behavioral alterations in pSNL rats 8 weeks after surgery, including decreased rearing activity and increased inactive time in the EPM test. Prior investigations [36,37,44] have demonstrated that the smallest PV-positive neurons have spherical or ovoid somata, whereas the largest neurons have multipolar somata. PV-positive neurons have four to five aspiny dendrites with sparse branching, and the width and length of these dendrites are often proportional to the size of their cell bodies [36]. Such distinct morphological characteristics may correspond to functionally

Table 4
Correlation table of behavior parameters and densities of c-Fos-, PV-positive neurons in subregions at 8 weeks after surgery.

	LA		**BLA**		**CA1**		**CA2**	
	c-Fos (+)	PV (+)	c-Fos (+)	PV (+)	c-Fos (+)	PV (+)	c-Fos (+)	PV (+)
OF$^{(B)}$	-0.70 *	0.59 *	-0.75 * *	0.65 *	-0.49	-0.62 *	-0.69	-0.62 *
	0.011	*0.044*	*0.005*	*0.023*	*0.106*	*0.031*	*0.14*	*0.033*
EPM$^{(A)}$	-0.77 * *	0.67 *	-0.73 * *	0.79 * *	-0.71 * *	-0.69 *	-0.64 *	-0.84 * *
	0.003	*0.018*	*0.007*	*0.003*	*0.009*	*0.012*	*0.024*	*0.001*

Data represent Spearman's rank correlation (upper) and p-value (lower).
OF$^{(B)}$: Percentage of rearing in center area.
EPM$^{(A)}$: Time spent in open arms.
*; * * Significant at the α level of 0.05 and 0.01 (2-tailed).

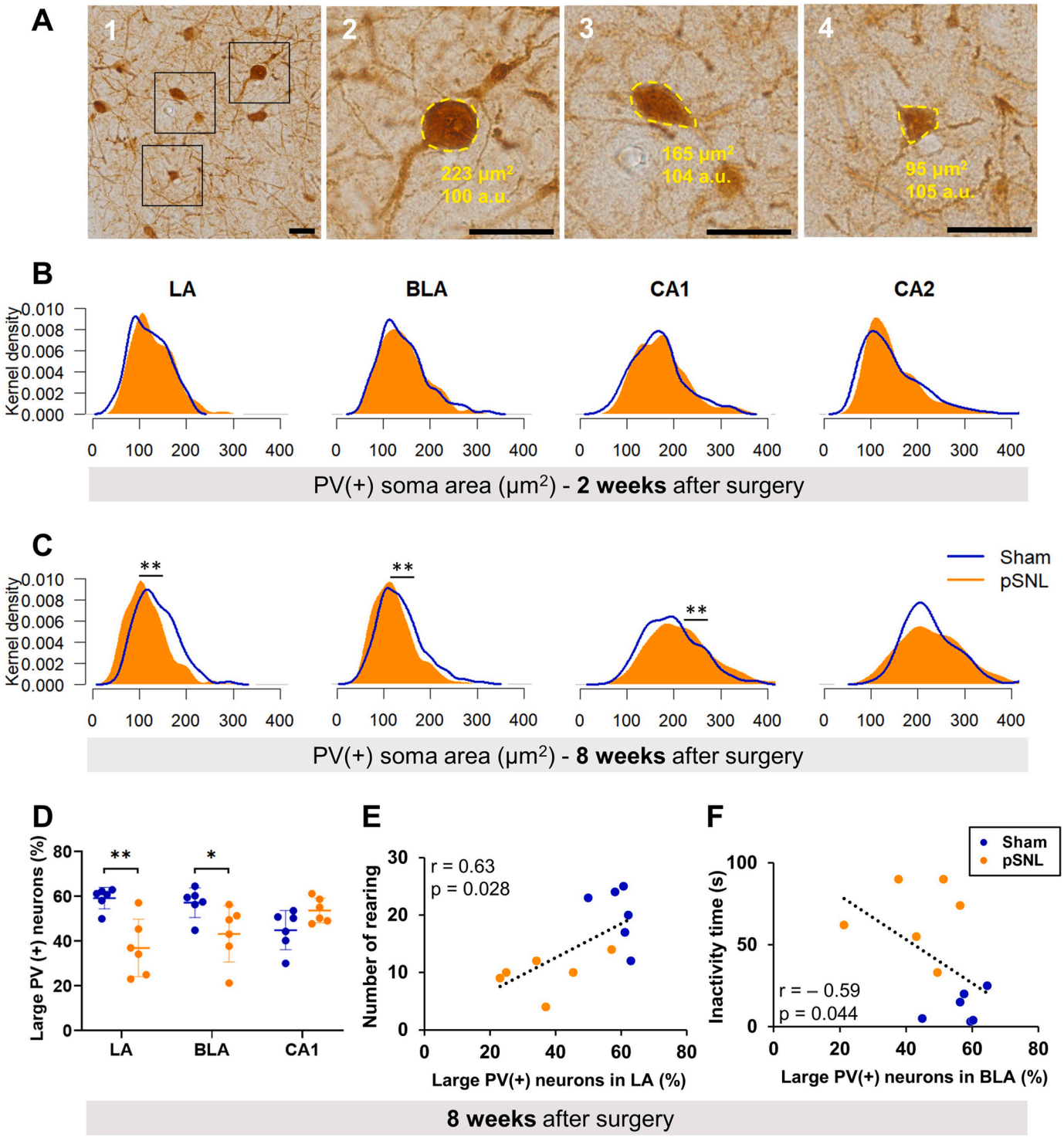

Fig. 6. Characteristics of PV-positive neuron somata size. (A) Representative images of PV-positive neurons in BLA (1); greater magnification was used to measure the soma area (2, 3, 4), scale bar = 25 μm. Yellow numbers indicate somata size and cell intensity. Distribution of PV-positive neuron somata area using kernel density estimation in some subregions of sham and pSNL rats at 2 weeks (B) and 8 weeks (C) after surgery. Kolmogorov–Smirnov tests were used to assess disparities in the distribution of the PV-positive neuron somata area between groups using cells as the statistical units. (D) Comparison of the percentage of large PV-positive neurons among the groups at 8 weeks after surgery (Mann—Whitney U test). (E, F) Correlation between the percentage of large PV-positive neurons and behavior parameters (Spearman's rank correlation). Significant difference from sham rats: *p < 0.05, * *p < 0.001. pSNL, partial sciatic nerve ligation; PV, parvalbumin; LA, lateral amygdala; BLA, basolateral amygdala; CA1–2, cornu ammonis areas 1–2; a.u, arbitraty unit.

segregated subpopulations, potentially reflecting differences in their electrophysiological properties [45]. Despite substantial variations in physical size over time and across a population, excitable cells manage to preserve their physiological properties and the electrical properties of cells exhibit high sensitivity to both membrane area and channel density [46]. Dendritic growth, concomitant with synaptic strengthening, leads to heightened neuronal activity [47]. Intriguingly, an increase in the number of small PV-positive neurons in the BLA is related to a reduction

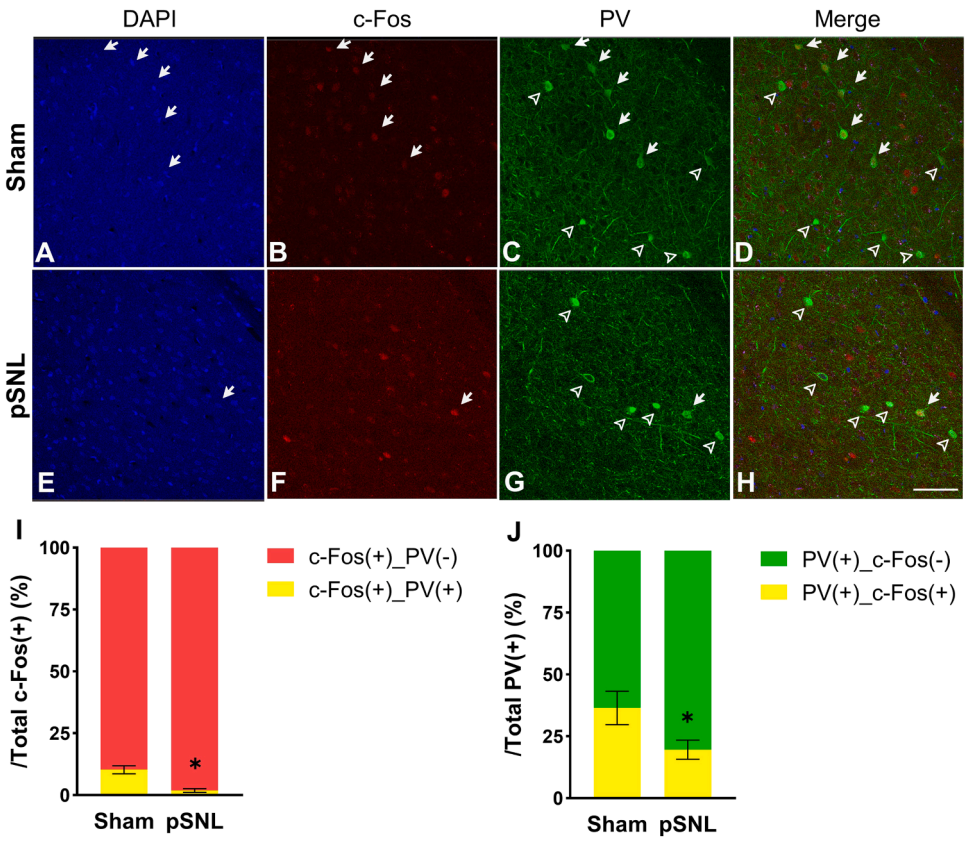

Fig. 7. Double immunofluorescence staining for c-Fos and PV in the basolateral amygdala of rats 8 weeks after surgery. DAPI labeling of cell nuclei (A and E), c-Fos-positive neurons (B and F), PV-positive neurons (C and G), and merged images (D and H). Arrows, cells coexpressing both PV and c-Fos; arrowheads, cells coexpressing PV only; scale bars = 50 μm. (I) Percentages of c-Fos-positive neurons coexpressing PV in total c-Fos-positive neurons. (J) Percentages of PV-positive neurons coexpressing c-Fos in total PV-positive neurons. Data are presented as mean ± standard error of the mean. Significant difference from sham rats: *$p < 0.05$, Mann—Whitney U test. DAPI, 4′,6-diamino-2-phenylindole labeling of cell nuclei; PV, parvalbumin; pSNL, partial sciatic nerve ligation.

in anxiety-like behavior in rodents exposed to an enriched environment [37]. Hence, the morphological differences between large and small PV-positive neurons in the amygdala indicate distinct functional roles related to emotional phenotypes that need further studies for confirmation.

In the present study, the proportion of activated PV-positive neurons in the amygdala of pSNL rats at 8 weeks after surgery decreased alongside the number of PV-positive neurons. This finding provides additional insights into the effect of altered PV-positive neuronal populations on amygdala function. The BLA is predominantly composed of glutamatergic (91%) and GABAergic (9%) neurons [48], with approximately half of the GABAergic neurons being PV-positive neurons [49]. Here, we observed more intense neuronal immunoreactivity with *c-Fos*, a marker of neuronal activation, and a reduction in the number of neurons coexpressing PV and *c-Fos* in the basolateral amygdaloid complex of pSNL rats with pain-induced anxiety-like behaviors. This suggests that the majority of single *c-Fos*-positive neurons in the BLA correspond to activated glutamatergic neurons. In mice with pain, the activation of glutamatergic neurons in the BLA in response to anxiety-inducing environments has been reported [50]. Moreover, the abnormal regulation of PV-positive neurons in the anterior BLA has been linked to the pathogenesis of prolonged anxiety states [51]. Reduced PV-positive neuronal activity has been observed in the BLA of rodents exposed to repeated restraint [52] and acute stress [53]. Therefore, an imbalance in the activity of PV-positive and projection neurons is likely to contribute to the promotion of anxiety-like behavior in pSNL rats.

The mechanisms underlying the alterations in PV-positive neurons in chronic pain are not fully understood, but some potential mechanisms have been proposed. A partial phenotypic shift, in which some PV-negative immunoreactive neurons adopt a PV-positive phenotype, could explain the increase in the number of PV-positive neurons. Reductions in the number of PV-positive neurons have been a subject of debate, with potential explanations ranging from PV cell mortality to impaired maturation or decreased PV expression [13]. Inflammation and oxidative stress have been implicated in the changes observed in PV-positive neurons [54–56]. Rats with nerve injury often have increased levels of reactive oxygen species, which can contribute to the development and maintenance of neuropathic pain [57,58]. Additionally, there is an increase in the glucocorticoid responsiveness of the hypothalamic–pituitary—adrenal axis in pain conditions, further suggesting the involvement of stress-related mechanisms. Oxidative stress has been associated with alterations in hippocampal PV-positive neurons in rats with anxiety [55]. In addition, the glucocorticoid hormone corticosterone has been shown to significantly reduce the number of PV-positive neurons. In the present study, we did not measure inflammatory biomarkers and stress-related hormones; however, widespread pathologies associated with chronic pain may have contributed to the alterations observed in PV-positive neurons in pSNL rats.

CCK could regulate activities of several types of neurons in a cell type-specific manner via interactions with GABA and endocannabinoid systems [59]. In mice, chemogenetic activation of CCK-positive inhibitory neurons globally increases anxiety-like behavior in the elevated plus maze test [60], whereas CCK knockdown in the BLA reduces anxiety-like behavior [61]. CCK injections into the cerebral ventricle induce anxiety through the CCK-2 receptor activation [62]. Although CCK-positive neurons have been previously reported to be involved in anxiety-like behaviors in rats with type 2 diabetes [19–21], no significant relationship between CCK-positive neuron density and anxiety-like

behaviors was observed in pSNL rats. Discrepancies may arise from variations in animal strain, stress models, and age at assessment between studies, with OLETF and Wistar rats, different stress models, and 20-week-old versus 17-week-old pSNL rats, respectively.

In this study, we analyzed the number of PV-positive neurons, the size of their somata, and the activation status in specific corticolimbic regions during two distinct phases: the early phase (2 weeks after surgery), prior to the onset of anxiety disorder, and the later phase (8 weeks after surgery), when anxiety disorder had already manifested and was notably intensified. More time points for morphological analysis could provide more conclusive evidence regarding the time course of changes in PV-positive neurons after surgery and their relationship with emerging anxiety-like behavior. Additionally, to elucidate the cellular mechanisms underlying anxiety-like behaviors in pSNL rats, the additional characteristics of PV-positive neurons and the direct interaction between PV-positive neurons and projection neurons should be examined using both anatomical and physiological approaches.

5. Conclusions

The present study revealed that rats with pSNL, which serve as a model for neuropathic pain, exhibit anxiety-like behaviors during the later phase of pain progression, but not during the earlier phase. These behavioral modifications are associated with changes in the density of PV-positive neurons in the LA and BLA and hippocampal CA1 and CA2 regions. In the basolateral amygdaloid complex of pSNL rats, 8 weeks after surgery, the observed changes in PV-positive neurons occurred primarily within the large cell subtypes, and the proportion of activated PV-positive neurons decreased. These results shed light on the potential role of PV-positive neurons in pain-induced anxiety-like behaviors.

Funding

This work was supported by a Grant-in-Aid for Scientific Research from the Japanese Ministry of Education, Culture, Sports, Science, and Technology (17K01503 and 23K10503; SU), and research funds from Hiroshima University. The funders had no role in study design, the collection, analysis, and interpretation of data, and the decision to submit the article for publication.

CRediT authorship contribution statement

Thu Nguyen Dang: Conceptualization, Data curation, Formal analysis, Investigation, Methodology, Writing - original draft, Writing - review & editing. **Son Nguyen Tien:** Conceptualization, Investigation, Methodology, Writing - review & editing. **Ryosuke Ochi:** Investigation, Methodology, Writing – review & editing. **Duc Le Trung:** Visualization, Writing - review & editing. **Kyo Nishio:** Data curation, Investigation. **Hiroki Kuwamura:** Visualization. **Tomoyuki Kurose:** Methodology, Writing – review & editing. **Naoto Fujita:** Methodology, Writing – review & editing. **Hisao Nishijo:** Methodology, Writing – review & editing. **Yoki Nakamura:** Conceptualization, Writing – review & editing. **Kazue Hisaoka-Nakashima:** Conceptualization, Writing – review & editing. **Norimitsu Morioka:** Conceptualization, Supervision, Writing – review & editing. **Susumu Urakawa:** Conceptualization, Formal analysis, Funding acquisition, Investigation, Methodology, Project administration, Supervision, Writing – original draft, Writing – review & editing.

Disclosure of interest

The authors declare that they have no competing interests.

Data Availability

Data will be made available on request.

Acknowledgments

A part of this work was carried out at the Analysis Center of Life Science, Natural Science Center for Basic Research and Development, Hiroshima University.

Appendix A. Supporting information

Supplementary data associated with this article can be found in the online version at doi:10.1016/j.bbr.2023.114786.

References

[1] S.P. Cohen, L. Vase, W.M. Hooten, Chronic pain: an update on burden, best practices, and new advances, Lancet 397 (10289) (2021) 2082–2097, https://doi.org/10.1016/s0140-6736(21)00393-7.
[2] A.M. Velly, S. Mohit, Epidemiology of pain and relation to psychiatric disorders, Prog. Neuropsychopharmacol. Biol. Psychiatry 87 (Pt B) (2018) 159–167, https://doi.org/10.1016/j.pnpbp.2017.05.012.
[3] O. Gureje, M. Von Korff, G.E. Simon, R. Gater, Persistent pain and well-being: a World Health Organization Study in Primary Care, JAMA 280 (2) (1998) 147–151, https://doi.org/10.1001/jama.280.2.147.
[4] S.E.E. Mills, K.P. Nicolson, B.H. Smith, Chronic pain: a review of its epidemiology and associated factors in population-based studies, Br. J. Anaesth. 123 (2) (2019) e273–e283, https://doi.org/10.1016/j.bja.2019.03.023.
[5] R. Melzack, From the gate to the neuromatrix, Pain. Suppl. 6 (1999) S121–S126, https://doi.org/10.1016/s0304-3959(99)00145-1.
[6] B. McCarberg, J. Peppin, Pain pathways and nervous system plasticity: learning and memory in pain, Pain. Med. 20 (12) (2019) 2421–2437, https://doi.org/10.1093/pm/pnz017.
[7] S. Bourne, A.G. Machado, S.J. Nagel, Basic anatomy and physiology of pain pathways, Neurosurg. Clin. N. Am. 25 (4) (2014) 629–638, https://doi.org/10.1016/j.nec.2014.06.001.
[8] D.D. Price, Psychological and neural mechanisms of the affective dimension of pain, Science 288 (5472) (2000) 1769–1772, https://doi.org/10.1126/science.288.5472.1769.
[9] N.T. Fiore, S.R. Debs, J.P. Hayes, S.S. Duffy, G. Moalem-Taylor, Pain-resolving immune mechanisms in neuropathic pain, Nat. Rev. Neurol. 19 (4) (2023) 199–220, https://doi.org/10.1038/s41582-023-00777-3.
[10] L.E. Potter, J.W. Paylor, J.S. Suh, G. Tenorio, J. Caliaperumal, F. Colbourne, G. Baker, I. Winship, B.J. Kerr, Altered excitatory-inhibitory balance within somatosensory cortex is associated with enhanced plasticity and pain sensitivity in a mouse model of multiple sclerosis, J. Neuroinflamm. 13 (1) (2016), 142, https://doi.org/10.1186/s12974-016-0609-4.
[11] H. Hu, J. Gan, P. Jonas, Interneurons. Fast-spiking, parvalbumin+ GABAergic interneurons: from cellular design to microcircuit function, Science 345 (6196) (2014), 1255263, https://doi.org/10.1126/science.1255263.
[12] J.A. Brown, T.S. Ramikie, M.J. Schmidt, R. Báldi, K. Garbett, M.G. Everheart, L. E. Warren, L. Gellért, S. Horváth, S. Patel, K. Mirnics, Inhibition of parvalbumin-expressing interneurons results in complex behavioral changes, Mol. Psychiatry 20 (12) (2015) 1499–1507, https://doi.org/10.1038/mp.2014.192.
[13] G. Perlman, A. Tanti, N. Mechawar, Parvalbumin interneuron alterations in stress-related mood disorders: a systematic review, Neurobiol. Stress 15 (2021), 100380, https://doi.org/10.1016/j.ynstr.2021.100380.
[14] J.B. Ruden, L.L. Dugan, C. Konradi, Parvalbumin interneuron vulnerability and brain disorders, Neuropsychopharmacology 46 (2) (2021) 279–287, https://doi.org/10.1038/s41386-020-0778-9.
[15] K. Miyahara, H. Nishimaru, J. Matsumoto, T. Setogawa, T. Taguchi, T. Ono, H. Nishijo, Involvement of parvalbumin-positive neurons in the development of hyperalgesia in a mouse model of fibromyalgia, Front. Pain. Res. 2 (2021), 627860, https://doi.org/10.3389/fpain.2021.627860.
[16] P. Juarez, V. Martínez Cerdeño, Parvalbumin and parvalbumin chandelier interneurons in autism and other psychiatric disorders, Front. Psychiatry 13 (2022), 913550, https://doi.org/10.3389/fpsyt.2022.913550.
[17] F. Mascagni, A.J. McDonald, Immunohistochemical characterization of cholecystokinin containing neurons in the rat basolateral amygdala, Brain Res. 976 (2) (2003) 171–184, https://doi.org/10.1016/s0006-8993(03)02625-8.
[18] T.A. Lovick, Pro-nociceptive action of cholecystokinin in the periaqueductal grey: a role in neuropathic and anxiety-induced hyperalgesic states, Neurosci. Biobehav. Rev. 32 (4) (2008) 852–862, https://doi.org/10.1016/j.neubiorev.2008.01.003.
[19] R. Ochi, N. Fujita, N. Goto, K. Takaishi, T. Oshima, S.T. Nguyen, H. Nishijo, S. Urakawa, Medial prefrontal area reductions, altered expressions of cholecystokinin, parvalbumin, and activating transcription factor 4 in the corticolimbic system, and altered emotional behavior in a progressive rat model of type 2 diabetes, PloS One 16 (9) (2021), e0256655, https://doi.org/10.1371/journal.pone.0256655.
[20] R. Ochi, N. Fujita, N. Goto, S.T. Nguyen, D.T. Le, K. Matsushita, T. Ono, H. Nishijo, S. Urakawa, Region-specific brain area reductions and increased cholecystokinin positive neurons in diabetic OLETF rats: implication for anxiety-like behavior, J. Physiol. Sci. 70 (1) (2020), 42, https://doi.org/10.1186/s12576-020-00771-0.
[21] R. Ochi, N. Fujita, K. Takaishi, T. Oshima, S.T. Nguyen, H. Nishijo, S. Urakawa, Voluntary exercise reverses social behavior deficits and the increases in the

densities of cholecystokinin-positive neurons in specific corticolimbic regions of diabetic OLETF rats, Behav. Brain Res. 428 (2022), 113886, https://doi.org/10.1016/j.bbr.2022.113886.
[22] Z. Seltzer, R. Dubner, Y. Shir, A novel behavioral model of neuropathic pain disorders produced in rats by partial sciatic nerve injury, Pain 43 (2) (1990) 205–218, https://doi.org/10.1016/0304-3959(90)91074-s.
[23] K.J. Kim, Y.W. Yoon, J.M. Chung, Comparison of three rodent neuropathic pain models, Exp. Brain Res. 113 (2) (1997) 200–206, https://doi.org/10.1007/bf02450318.
[24] J. Simpson, J.P. Kelly, An investigation of whether there are sex differences in certain behavioural and neurochemical parameters in the rat, Behav. Brain Res. 229 (1) (2012) 289–300, https://doi.org/10.1016/j.bbr.2011.12.036.
[25] J.C. Morales-Medina, M.A. Bautista-Carro, G. Serrano-Bello, P. Sánchez-Teoyotl, A. G. Vásquez-Ramírez, T. Iannitti, Persistent peripheral inflammation and pain induces immediate early gene activation in supraspinal nuclei in rats, Behav. Brain Res. 446 (2023), 114395, https://doi.org/10.1016/j.bbr.2023.114395.
[26] T.L. Krukoff, c-fos expression as a marker of functional activity in the brain, in: A. A. Boulton, G.B. Baker, A.N. Bateson (Eds.), Cell Neurobiology Techniques, Humana Press, Totowa, NJ, 1999, pp. 213–230.
[27] M.W. Hale, J.A. Bouwknecht, F. Spiga, A. Shekhar, C.A. Lowry, Exposure to high- and low-light conditions in an open-field test of anxiety increases c-Fos expression in specific subdivisions of the rat basolateral amygdaloid complex, Brain Res. Bull. 71 (1–3) (2006) 174–182, https://doi.org/10.1016/j.brainresbull.2006.09.001.
[28] M.S. Minett, K. Quick, J.N. Wood, Behavioral measures of pain thresholds, Curr. Protoc. Mouse Biol. 1 (3) (2011) 383–412, https://doi.org/10.1002/9780470942390.mo110116.
[29] M. Gulyás, N. Bencsik, S. Pusztai, H. Liliom, K. Schlett, AnimalTracker: an ImageJ-based tracking API to create a customized behaviour analyser program, Neuroinformatics 14 (4) (2016) 479–481, https://doi.org/10.1007/s12021-016-9303-z.
[30] M. Casarrubea, J.B. Leca, N. Gunst, G.K. Jonsson, M. Portell, G. Di Giovanni, S. Aiello, G. Crescimanno, Structural analyses in the study of behavior: from rodents to non-human primates, Front Psychol. 13 (2022), 1033561, https://doi.org/10.3389/fpsyg.2022.1033561.
[31] E. Choleris, A.W. Thomas, M. Kavaliers, F.S. Prato, A detailed ethological analysis of the mouse open field test: effects of diazepam, chlordiazepoxide and an extremely low frequency pulsed magnetic field, Neurosci. Biobehav. Rev. 25 (3) (2001) 235–260, https://doi.org/10.1016/s0149-7634(01)00011-2.
[32] P.-O. Montiglio, D. Garant, D. Thomas, D. Réale, Individual variation in temporal activity patterns in open-field tests, Anim. Behav. 80 (5) (2010) 905–912, https://doi.org/10.1016/j.anbehav.2010.08.014.
[33] C.W. George Paxinos. The Rat Brain in Stereotaxic Coordinates, seventh ed., Elsevier Academic Press, 2013.
[34] P.E. Wainwright, S. Lévesque, L. Krempulec, B. Bulman-Fleming, D. McCutcheon, Effects of environmental enrichment on cortical depth and Morris-maze performance in B6D2F2 mice exposed prenatally to ethanol, Neurotoxicol. Teratol. 15 (1) (1993) 11–20, https://doi.org/10.1016/0892-0362(93)90040-u.
[35] D. Xia, L. Li, B. Yang, Q. Zhou, Altered relationship between parvalbumin and perineuronal nets in an autism model, Front Mol. Neurosci. 14 (2021), 597812, https://doi.org/10.3389/fnmol.2021.597812.
[36] S. Kemppainen, A. Pitkänen, Distribution of parvalbumin, calretinin, and calbindin-D(28k) immunoreactivity in the rat amygdaloid complex and colocalization with gamma-aminobutyric acid, J. Comp. Neurol. 426 (3) (2000) 441–467, https://doi.org/10.1002/1096-9861(20001023)426:3<441::aid-cne8>3.0.co;2-7.
[37] S. Urakawa, K. Takamoto, E. Hori, N. Sakai, T. Ono, H. Nishijo, Rearing in enriched environment increases parvalbumin-positive small neurons in the amygdala and decreases anxiety-like behavior of male rats, BMC Neurosci. 14 (2013), 13, https://doi.org/10.1186/1471-2202-14-13.
[38] M. Casarrubea, V. Roy, F. Sorbera, M.S. Magnusson, A. Santangelo, A. Arabo, G. Crescimanno, Temporal structure of the rat's behavior in elevated plus maze test, Behav. Brain Res. 237 (2013) 290–299, https://doi.org/10.1016/j.bbr.2012.09.049.
[39] H. Ueno, K. Takao, S. Suemitsu, S. Murakami, N. Kitamura, K. Wani, M. Okamoto, S. Aoki, T. Ishihara, Age-dependent and region-specific alteration of parvalbumin neurons and perineuronal nets in the mouse cerebral cortex, Neurochem. Int. 112 (2018) 59–70, https://doi.org/10.1016/j.neuint.2017.11.001.
[40] G. Mascio, S. Notartomaso, K. Martinello, F. Liberatore, D. Bucci, T. Imbriglio, M. Cannella, N. Antenucci, P. Scarselli, R. Lattanzi, V. Bruno, F. Nicoletti, S. Fucile, G. Battaglia, A progressive build-up of perineuronal nets in the somatosensory cortex is associated with the development of chronic pain in mice, J. Neurosci. 42 (14) (2022) 3037–3048, https://doi.org/10.1523/jneurosci.1714-21.2022.
[41] M.D.J. Seno, D.V. Assis, F. Gouveia, G.F. Antunes, M. Kuroki, C.C. Oliveira, L.C. T. Santos, R.L. Pagano, R.C.R. Martinez, The critical role of amygdala subnuclei in nociceptive and depressive-like behaviors in peripheral neuropathy, Sci. Rep. 8 (1) (2018), 13608, https://doi.org/10.1038/s41598-018-31962-w.
[42] Z.Y. Luo, L. Huang, S. Lin, Y.N. Yin, W. Jie, N.Y. Hu, Y.Y. Hu, Y.F. Guan, J.H. Liu, Q.L. You, Y.H. Chen, Z.C. Luo, S.R. Zhang, X.W. Li, J.M. Yang, Y.M. Tao, L. Mei, T. M. Gao, Erbin in amygdala parvalbumin-positive neurons modulates anxiety-like behaviors, Biol. Psychiatry 87 (10) (2020) 926–936, https://doi.org/10.1016/j.biopsych.2019.10.021.
[43] M. Hamann, M. Bennay, M. Gernert, K. Schwabe, M. Koch, A. Richter, Decreased density of amygdaloid parvalbumin-positive interneurons and behavioral changes in dystonic hamsters (Mesocricetus auratus), Behav. Neurosci. 122 (1) (2008) 36–43, https://doi.org/10.1037/0735-7044.122.1.36.
[44] A.J. McDonald, R.L. Betette, Parvalbumin-containing neurons in the rat basolateral amygdala: morphology and co-localization of Calbindin-D(28k), Neuroscience 102 (2) (2001) 413–425, https://doi.org/10.1016/s0306-4522(00)00481-4.
[45] D.G. Rainnie, I. Mania, F. Mascagni, A.J. McDonald, Physiological and morphological characterization of parvalbumin-containing interneurons of the rat basolateral amygdala, J. Comp. Neurol. 498 (1) (2006) 142–161, https://doi.org/10.1002/cne.21049.
[46] S. Gorur-Shandilya, E. Marder, T. O'Leary, Activity-dependent compensation of cell size is vulnerable to targeted deletion of ion channels, Sci. Rep. 10 (1) (2020), 15989, https://doi.org/10.1038/s41598-020-72977-6.
[47] M.F. Zwart, O. Randlett, J.F. Evers, M. Landgraf, Dendritic growth gated by a steroid hormone receptor underlies increases in activity in the developing Drosophila locomotor system, Proc. Natl. Acad. Sci. USA 110 (40) (2013) E3878-87., https://doi.org/10.1073/pnas.1311711110.
[48] A. Beyeler, J. Dabrowska, Neuronal diversity of the amygdala and the bed nucleus of the stria terminalis, Handb. Behav. Neurosci. 26 (2020) 63–100, https://doi.org/10.1016/b978-0-12-815134-1.00003-9.
[49] A.J. McDonald, F. Mascagni, Colocalization of calcium-binding proteins and GABA in neurons of the rat basolateral amygdala, Neuroscience 105 (3) (2001) 681–693, https://doi.org/10.1016/s0306-4522(01)00214-7.
[50] J. Liu, D. Li, J. Huang, J. Cao, G. Cai, Y. Guo, G. Wang, S. Zhao, X. Wang, S. Wu, Glutamatergic neurons in the amygdala are involved in paclitaxel-induced pain and anxiety, Front. Psychiatry 13 (2022), 869544, https://doi.org/10.3389/fpsyt.2022.869544.
[51] J.L. Lukkes, A.R. Burke, N.S. Zelin, M.W. Hale, C.A. Lowry, Post-weaning social isolation attenuates c-Fos expression in GABAergic interneurons in the basolateral amygdala of adult female rats, Physiol. Behav. 107 (5) (2012) 719–725, https://doi.org/10.1016/j.physbeh.2012.05.007.
[52] L.R. Reznikov, L.P. Reagan, J.R. Fadel, Activation of phenotypically distinct neuronal subpopulations in the anterior subdivision of the rat basolateral amygdala following acute and repeated stress, J. Comp. Neurol. 508 (3) (2008) 458–472, https://doi.org/10.1002/cne.21687.
[53] A. Guadagno, S. Verlezza, H. Long, T.P. Wong, C.D. Walker, It is all in the right amygdala: increased synaptic plasticity and perineuronal nets in male, but not female, juvenile rat pups after exposure to early-life stress, J. Neurosci. 40 (43) (2020) 8276–8291, https://doi.org/10.1523/jneurosci.1029-20.2020.
[54] X.R. Sun, H. Zhang, H.T. Zhao, M.H. Ji, H.H. Li, J. Wu, K.Y. Li, J.J. Yang, Amelioration of oxidative stress-induced phenotype loss of parvalbumin interneurons might contribute to the beneficial effects of environmental enrichment in a rat model of post-traumatic stress disorder, Behav. Brain Res. 312 (2016) 84–92, https://doi.org/10.1016/j.bbr.2016.06.016.
[55] A.R. Soares, K.R. Gildawie, J.A. Honeycutt, H.C. Brenhouse, Region-specific effects of maternal separation on oxidative stress accumulation in parvalbumin neurons of male and female rats, Behav. Brain Res. 388 (2020), 112658, https://doi.org/10.1016/j.bbr.2020.112658.
[56] J.L. Lukkes, S. Meda, B.S. Thompson, N. Freund, S.L. Andersen, Early life stress and later peer distress on depressive behavior in adolescent female rats: Effects of a novel intervention on GABA and D2 receptors, Behav. Brain Res. 330 (2017) 37–45, https://doi.org/10.1016/j.bbr.2017.04.053.
[57] H.K. Kim, S.K. Park, J.L. Zhou, G. Taglialatela, K. Chung, R.E. Coggeshall, J. M. Chung, Reactive oxygen species (ROS) play an important role in a rat model of neuropathic pain, Pain 111 (1–2) (2004) 116–124, https://doi.org/10.1016/j.pain.2004.06.008.
[58] J. Xu, S. Wu, J. Wang, J. Wang, Y. Yan, M. Zhu, D. Zhang, C. Jiang, T. Liu, Oxidative stress induced by NOX2 contributes to neuropathic pain via plasma membrane translocation of PKCε in rat dorsal root ganglion neurons, J. Neuroinflamm. 18 (1) (2021), 106, https://doi.org/10.1186/s12974-021-02155-6.
[59] C. Földy, S.Y. Lee, J. Szabadics, A. Neu, I. Soltesz, Cell type-specific gating of perisomatic inhibition by cholecystokinin, Nat. Neurosci. 10 (9) (2007) 1128–1130, https://doi.org/10.1038/nn1952.
[60] P.D. Whissell, J.Y. Bang, I. Khan, Y.F. Xie, G.M. Parfitt, M. Grenon, N.W. Plummer, P. Jensen, R.P. Bonin, J.C. Kim, Selective activation of cholecystokinin-expressing GABA (CCK-GABA) neurons enhances memory and cognition, eNeuro 6 (1) (2019), https://doi.org/10.1523/eneuro.0360-18.2019.
[61] C. Del Boca, P.E. Lutz, J. Le Merrer, P. Koebel, B.L. Kieffer, Cholecystokinin knock-down in the basolateral amygdala has anxiolytic and antidepressant-like effects in mice, Neuroscience 218 (2012) 185–195, https://doi.org/10.1016/j.neuroscience.2012.05.022.
[62] L. Singh, A.S. Lewis, M.J. Field, J. Hughes, G.N. Woodruff, Evidence for an involvement of the brain cholecystokinin B receptor in anxiety, Proc. Natl. Acad. Sci. USA 88 (4) (1991) 1130–1133, https://doi.org/10.1073/pnas.88.4.1130.